chemengineering

MDPI

Article

Natural Hematite and Siderite as Heterogeneous Catalysts for an Effective Degradation of 4-Chlorophenol via Photo-Fenton Process

Haithem Bel Hadjltaief [1], Ali Sdiri [1], María Elena Gálvez [2,*], Haythem Zidi [1], Patrick Da Costa [2] and Mourad Ben Zina [1]

[1] Laboratory of Water, Energy and Environment, National Engineering School, University of Sfax, P.O. Box 1173 W, 3038 Sfax, Tunisia; bel_hadj22@yahoo.com (H.B.H.); ali.sdiri@enis.rnu.tn (A.S.); zidi.haytham@gmail.com (H.Z.); Mourad.Benzina@enis.rnu.tn (M.B.Z.)

[2] CNRS, Institut Jean Le Rond d'Alembert, Sorbonne Université, 2 place de la gare de ceinture, 78210 Saint-Cyr-L'Ecole, France; patrick.da_costa@upmc.fr

* Correspondence: elena.galvez_parruca@upmc.fr; Tel.: +33-1-30-85-48-77

Received: 18 May 2018; Accepted: 9 June 2018; Published: 21 June 2018

Abstract: This paper describes a simple and low-cost process for the degradation of 4-Chlorophenol (4-CP) from aqueous solution, using natural Tunisian Hematite (M_1) and Siderite (M_2). Two natural samples were collected in the outcroppings of the Djerissa mining site (Kef district, northwestern Tunisia). Both Hematite and Siderite ferrous samples were characterized using several techniques, including X-Ray Diffraction (XRD), Nitrogen Physisorption (BET), Infrared Spectroscopy (FTIR), H_2-Temperature Programmed Reduction (H_2-TPR), Scanning Electronic Microscopy (SEM) linked with Energy Dispersive X-ray (EDS) and High-Resolution Transmission Electron Microscopy (HRTEM). Textural, structural and chemical characterization confirmed the presence of Hematite and Siderite phases with a high amount of iron on the both surface materials. Their activity was evaluated in the oxidation of 4-CP in aqueous medium under heterogeneous photo-Fenton process. Siderite exhibited higher photocatalytic oxidation activity than Hematite at pH 3. The experimental results also showed that 100% conversion of 4-CP and 54% TOC removal can be achieved using Siderite as catalyst. Negligible metal leaching and catalyst reutilization without any loss of activity point towards an excellent catalytic stability for both natural catalysts.

Keywords: heterogeneous catalysts; photo-Fenton; hematite; siderite; oxidation; 4-chlorophenol

1. Introduction

The phenol-derivate 4-chlorophenol (4-CP) is a widely used both as a solvent and as a platform molecule in the synthesis of dyes, insecticides, pesticides, biocides, paints, phenolic resins, plastics and other chemicals [1–3]. Nevertheless, 4-CP is known for its carcinogenic and mutagenic effects [2]. 4-CP can result in respiratory tract irritation, in addition to its deleterious effects on eyes, skin and mucous membrane. According to the European Union standards, the threshold limit of total phenols in potable water is 0.5 mg/L [3,4]. Thus, it is fundamentally important to reduce phenol contents in both potable and wastewater. To achieve this goal, various methods have been developed, including adsorption [5], biological degradation [6], electrochemical oxidation [2], wet oxidation [4], photocatalytic degradation [1] and photo-Fenton oxidation [7–9]. A homogeneous Fenton or photo-Fenton reaction is considered one of the most promising ways to remove highly hazardous phenolic species, because it is not influenced by their toxicity [10,11]. Fenton oxidation is however not efficient enough at neutral pH. Moreover, the separation and regeneration of the catalyst

(homogeneous) and the possible secondary contamination due to the presence of 50–80 ppm iron in the treated effluent are important drawbacks for its scale-up and feasible application [11,12].

To overcome these disadvantages of homogeneous system, special attention has been given to the development heterogeneous Fe-catalyst. Different support materials, such as synthetic or natural zeolites, clays, polymers, silica, carbon or resins, have shown to be good candidates for the heterogenization of Fe-containing catalysts for the oxidative degradation of organic compounds through the Fenton or photo-Fenton reaction [13–15]. In addition, the so-prepared catalysts have generally shown an excellent catalytic activity and high stability. Nevertheless, they have high preparation cost via the use of chemicals, high-energy demands and calcinations.

In this context, the use of Natural clay-like heterogeneous materials such as hematite [11], pyrite and chalcopyrite [16], siderite [17], magnetite [18] and goethite [19] are alternative ecosystem friendly natural materials for the organic pollutants in water. In addition, their use as clay-like materials is gaining importance due to their high stability under irradiation, possibility of recovery and reuse while no strict control of the pH is required during the reactions [11,16–19]. Natural pyrite (FeS_2) and chalcopyrite ($CuFeS_2$) were used as heterogeneous Fenton catalyst for the degradation of phenolic compounds found in olive mill wastewater (OMW). The related results showed that high TOC removal, low leaching of iron species and spontaneous formation of a small amount of H_2O_2 under acid conditions [16]. In a subsequent work, the catalytic activity of Natural Tunisian clay-like material (i.e., Hematite) was also investigated in oxidation of phenol and 2-chlorophenol using heterogeneous photo-Fenton [11,20].

Since, generally, high content of iron oxides are needed, the use of environmentally friendly and more economical raw material may be a good option for the preparation of such Fe-catalysts. In this sense some natural Tunisian materials containing very important amounts of iron can be of considerable interest in photo-Fenton processes. Such materials can be directly used in heterogeneous Fenton applications, bypassing the need of employing any other Fe-source, as well as the catalyst preparation process itself. To the best of our knowledge and based on a detailed literature review, in the present work, we show for the first time that these materials (Hematite and Siderite) can be used as catalysts for the degradation of organic pollutants by means of photo-Fenton processes. In this sense, the main objective of the present work is to evaluate the activity of two raw Tunisian materials (i.e., Hematite (M_1) and Siderite (M_2)) in the degradation and mineralization of 4-chlorophenol in aqueous solution, considering as well its stability on a prolonged operation time.

2. Materials and Methods

2.1. Materials and Reagents

Raw ferrous samples M_1 and M_2 were collected from Djerissa mines, kef district, northwestern Tunisia (Figure 1). These materials were first crushed, dispersed and purified in water, and the desired particle size of less than 60 µm was extracted by simple sedimentation. This fraction was then ultrasonicated in 95% ethanol for 5 min, washed with 0.1 M HNO_3, rinsed with deionized water and 95% ethanol and finally dried to 30 °C. Hydrogen peroxide (35%), 4-Chlorophenol (>99%) and MnO_2 (>99%) were of analytical reagent grade, purchased from Sigma-Aldrich (now Merck KGaA, Darmstadt, Germany).

2.2. Physicochemical Characterization

Chemical composition of the both siderite and hematite samples was determined by X-ray fluorescence with an ARL® 9800 XP (Thermo Fischer Scientific, Waltham, MA, USA) spectrometer. Nitrogen adsorption–desorption isotherms were determined at −196 °C on a Micromeritics ASAP 2010 (Micromeritics Norcross, Norcross, GA, USA), after degassing (10^{-5} Pa) for 24 h at ambient temperature. Surface areas were calculated using the BET equation, whereas mean pore size, pore size distribution and pore volume were estimated using the BJH method.

Raw Material M_1 Raw Material M_2

Figure 1. Outcroppings of the materials in Jrissa mining site.

X-ray diffraction (XRD) patterns were obtained in a Philips® PW 1710 PAN (PAN Analytical, Almelo, The Netherlands) analytical Empyrean diffractometers equipped with Cu K_α (λ = 1.5406 Å) radiation source and 2θ range between 3° and 80°, with a step size of 0.02°/s.

The profiles of temperature-programmed reduction (H_2-TPR) were acquired in a BELCAT-M (BEL Japan) device, equipped with a thermal conductivity detector (TCD). The sample-based catalysts were first degassed to 100 °C for 2 h, and then reduced in 5% (vol.) H_2/Ar, while increasing temperature from 100 to 900 °C at a increment of 7.5 °C/min.

The morphology was ascertained using a scanning electron microscope (SEM, HitachiSU-70, Hitachi, Tokyo, Japan) equipped with an Oxford X-Max 50 mm^2 X-ray spectroscopy systems through dispersive energy (EDX), which enabled qualitative evaluation of chemical composition. High resolution transmission electron microscopy (HRTEM) images were also obtained on a JEOLJEM 2011 equipped with LaB_6 filament and operating at 200 kV. Images were collected with a 4008 × 2672 pixel CCD camera (Gatan Orius SC1000, Gatan, Pleasanton, CA, USA) coupled with DIGITAL MICROGRAPH software (GMS 3).

2.3. Photo-Fenton Experiments and Analytical Procedures

Heterogeneous photo-Fenton experiments were performed in an open Pyrex-glass cell (250 mL volume, 5 cm inner diameter and 11 cm height). A detailed description of catalytic reactor was reported by Bel Hadjltaief et al. [10,21]. Irradiation was carried out using 2 parallel UV lamps at 254 and 365 nm at 930/13 μW/cm^2. All of the experiments were performed keeping the distance between the solution and the lamps constant at 15 cm and under room temperature conditions (i.e., 25 °C). The initial pH of the 4-Chlorophenol solution was adjusted to acidic condition (pH = 3), optimum pH for photo-Fenton processes [22]. The initial concentration of 4-CP in the treated solution was 20 mg/L. After stabilization of the stirring (200 rpm), 0.05 g of catalyst was added to 100 mL of an aqueous 4-CP solution. Then, a fixed volume (2 mL) of a 1000 mg/L H_2O_2 solution was poured into the 4-CP solution. H_2O_2 addition was taken as the initial time of the reaction. Aliquots of supernatant (1 mL) were regularly extracted from the reaction vessel with the aid of a syringe; Residual H_2O_2 was immediately quenched with MnO_2 (99% Merck) to prevent the dark Fenton reaction occurring through the possible presence of leached iron. Before analysis, the liquid was filtered using PTFE filters (0.45 μm). In addition, the liquid solutions after reactions were analyzed by ICP-OES device to determine the iron content. The choice of these experimental conditions was based in the previous published papers on Fenton and photocatalysis using clay-derived catalysts.

The concentration of 4-chlorophenol in the solution was analyzed using an Agilent 2025 GC (Agilent, Santa Clara, CA, USA) gas chromatography (GC), equipped with a Zebron capillary column ZB-5MSi (30 m × 0.32 mm × 0.25 μm) and a flame ionization detector (FID). The extent of the

mineralization of the 4-CP was determined based on total organic carbon measurements using a Shimadzu TOC-5000A (Shimadzu, Kyoto, Japan) analyzer. Degradation and mineralization efficiencies were calculated as follows:

$$\text{Degradation/mineralization efficiency} = ((C_0 - C_t)/C_0) \times 100 \quad (1)$$

where C_t denotes the time-dependent concentration/TOC and C_0 is the initial concentration/TOC. Note here that the degradation experiments were repeated three times to check the repeatability of the results obtained.

3. Results and Discussion

3.1. Catalysts Characterization

Chemical composition of the raw materials M_1 and M_2 was comparable, but M_1 had a distinctly higher content of iron (Table 1). High amount of iron was found used in heterogeneous photo-Fenton oxidation of 4-CP. Nitrogen adsorption–desorption isotherms of both catalysts are given in Figure 2. The isotherm exhibited a typical International Union of Pure and Applied Chemistry (IUPAC) type IV with a tight hysteresis loop at high relative pressure (p/p_0 = 0.4–1.0); this indicated the presence of laminar-structured materials containing slit-shaped mesopores [11]. As shown in Table 2, the specific surface area (S_{BET}), pore volume and average pore diameter for M_2 are higher than that of M_1.

Table 1. Chemical composition (percent oxides, X-ray fluorescence) of the two raw materials.

Samples	SiO_2	Al_2O_3	Fe_2O_3	CaO	MgO	MnO	K_2O	PF
M_1	9.45	2.91	46.89	5.38	4.35	0.26	0.13	31.54
M_2	7.63	0.94	57.6	2.93	2.2	0.22	0.14	28.53

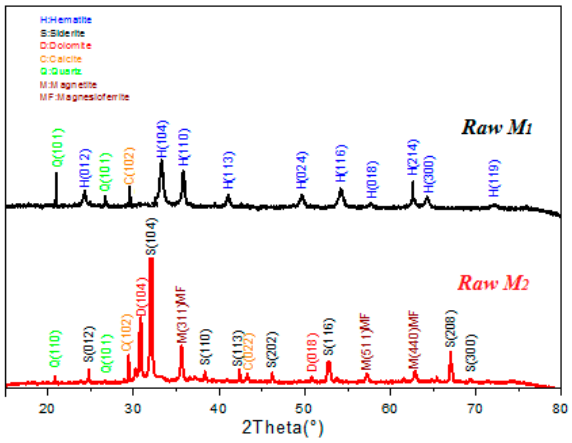

Figure 2. XRD patterns for the raw materials M_1 and M_2.

Table 2. Textural properties of the two raw materials.

Samples	Surface Area ($m^2\ g^{-1}$)	Mean Pore Size (nm)	Pore Volume ($cm^3\ g^{-1}$)
M_1	8.00	16.1	0.03
M_2	37.5	8.00	0.07

Figure 3 depicts the mineralogical analysis and phase structures of M_1 and M_2 samples. The crystalline structure of the raw material M_1, identified by XRD measurement, showed the main crystalline phases of hematite; the main impurity was calcite and quartz. The XRD patterns of the M_1 showed

diffraction peaks near 2θ values of 24.3°, 33.3°, 35.81°, 41.08°, 49.6°, 54.18, 57.7°, 62.57°, 64.3° and 72.13° corresponding to (012), (104), (110), (113), (024), (116), (118), (214), (300) and (119) planes of the Hematite type, respectively (JCPDS card file No. 85-1575) [23]. Based on XRD data, siderite is the major mineralogical compound in the structure of natural material, along with quartz as minor compound (Figure 3). Peaks located at 24.7°, 32.2°, 38.4°, 42.4°, 46.2°, 50.8°, 52.3°, 60.9°, 64.6° and 65° indicated the presence of siderite, but those near 26.7 and 67 are indicative of quartz [24–26]. FT-IR spectra is given in Figure 4. It showed the presence of OH stretching bands near 1790 cm^{-1}, as well as the broad Si-O stretching band near 1000 cm^{-1} [27]. Vibration bands at 736 cm^{-1}, in the range 860–880 cm^{-1} and 1390–1440 cm^{-1} are attributed to the CO bond of the carbonates, confirming the results of XRD and chemical analyses (Siderite: $FeCO_3$, Calcite: $CaCO_3$ and Dolomite: $MgCa(CO_3)_2$). This latter result is in agreement with the literature [24,25,28,29]. TPR analysis was performed to get detailed information about the nature of the iron oxides. The reduction profile of the raw M_1 displayed two hydrogen consumption peaks in the range 200–800 °C, coinciding with the reduction profile of Fe_2O_3 [20]. As for M_2 sample, three reduction peaks were observed (Figure 5). An increase in temperature caused the dissociation of iron carbonates in iron oxides such as FeO and Fe_3O_4.

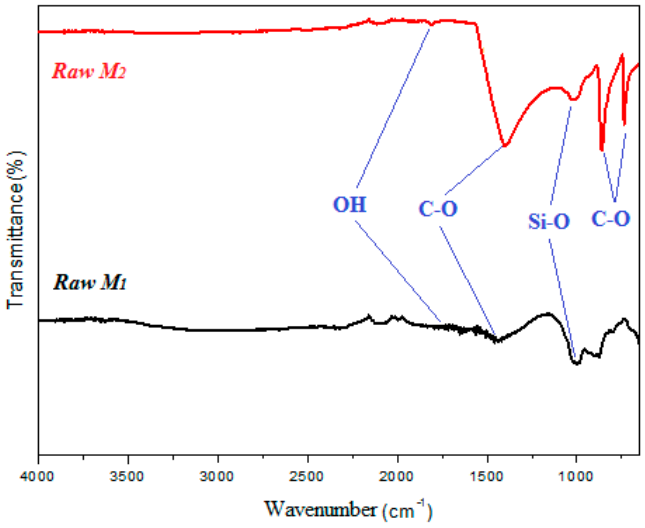

Figure 3. FT–IR spectra for the raw materials M_1 and M_2.

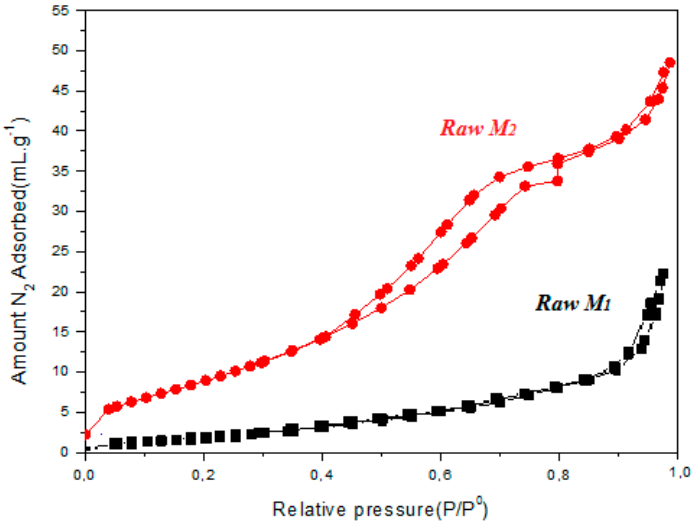

Figure 4. Nitrogen adsorption–desorption isotherms for raw materials M_1 and M_2.

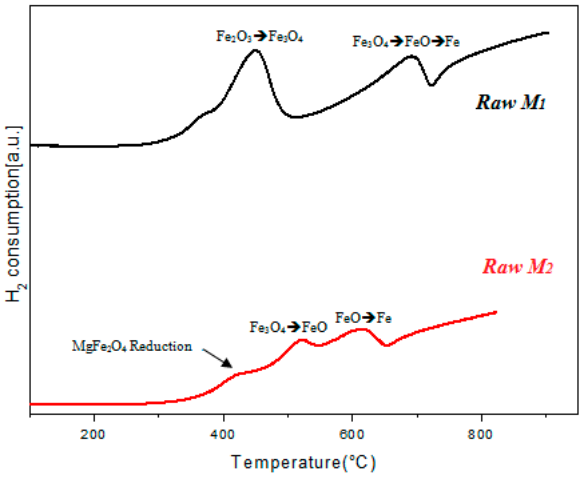

Figure 5. Temperature programmed reduction (H_2-TPR) profiles for raw materials M_1 and M_2.

SEM images are shown in Figure 6. They indicated spherical to sub-round particles with some agglomerated platelets for the raw M_1 sample. In contrast, M_2 sample is predominantly particles with some rhombohedral shapes. EDX analysis confirmed the presence of high amount of iron on the surface of both materials, with small amounts of impurities, e.g., Si, Al, Fe, Ca, Mg, and Mn, confirming the results of X-ray fluorescence. TEM images further confirmed these changes in the morphology of the M_1 and M_2 samples (Figure 7). Interlayer distances were measured from the Fast Fourier Transform (FFT) of the HRTEM image. For M_1, the presence of (012) planes with an inter-reticular distance of 3.65 Å characteristic of Hematite was clearly distinguished, whereas, for M_2, HRTEM images showed lattice fringes from which the (110) plane of siderite and (311) of Magnetite with the respective d-spacing of 2.3 and 2.5 Å.

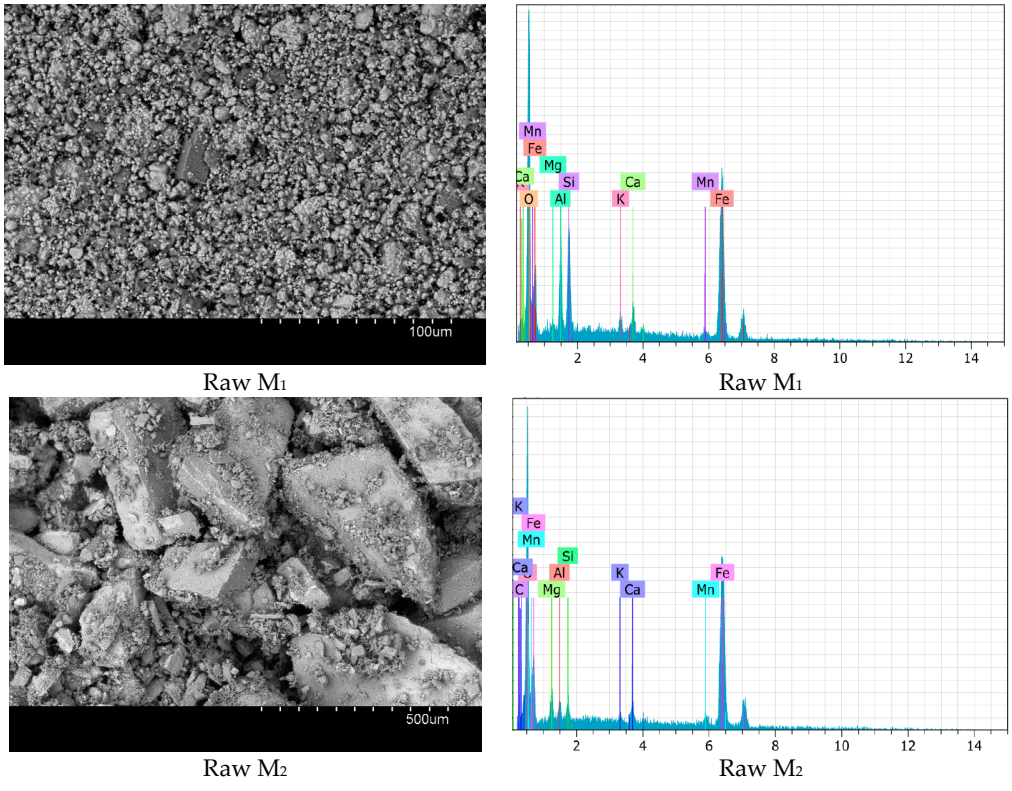

Figure 6. SEM images and EDX spectra for the raw materials M_1 and M_2.

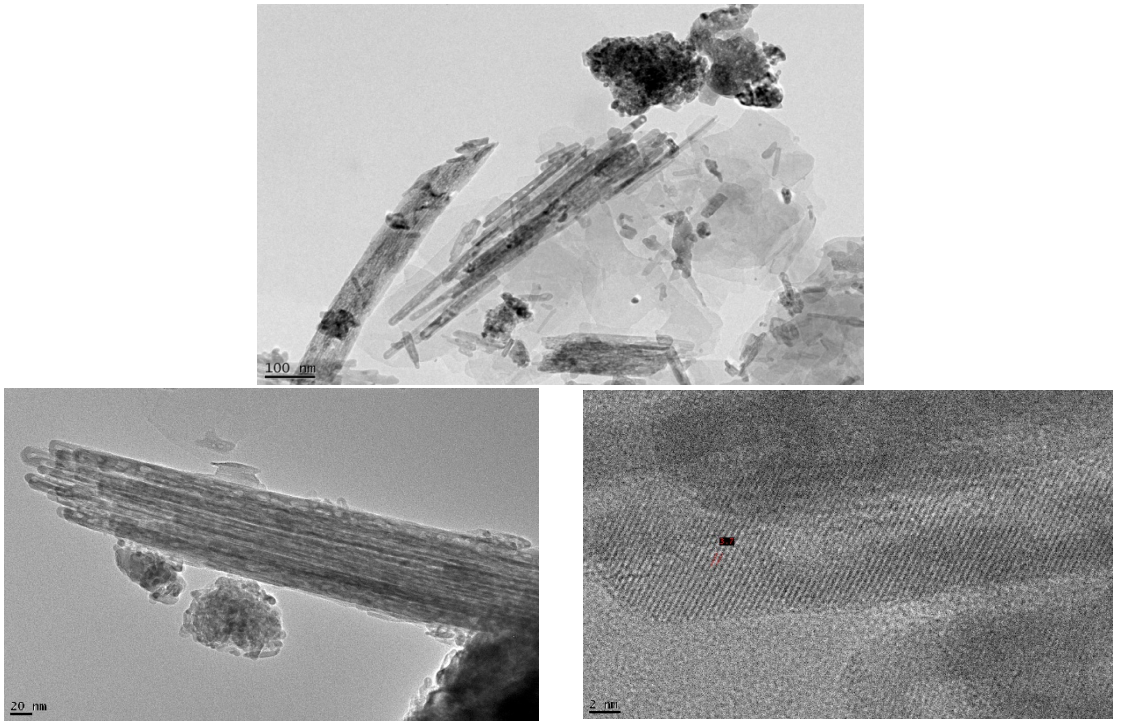

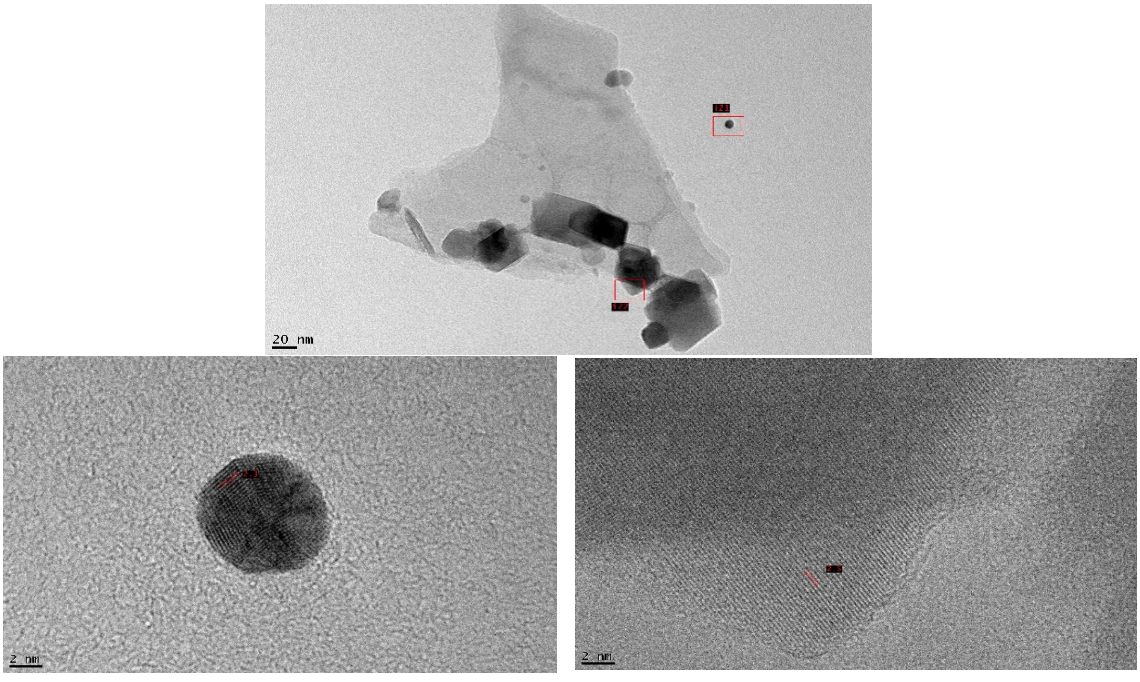

Figure 7. TEM images for the raw materials M_1 and M_2.

3.2. Catalytic Performance in the Photo-Fenton Oxidation of 4-Chlorophenol

Preliminary experiments were carried out to assess the importance of H_2O_2, catalysts and irradiation for 4-CP degradation. Insignificant degradation was observed under H_2O_2, 4-CP and both catalysts alone. In the dark condition, a mixture of H_2O_2 with catalysts showed 4-CP conversion of 52.1% and 40.3% for M_1 and M_2, respectively. This may indicate that Fenton reaction took place via the enhanced radical formation, which, in turn, was involved in the oxidation of organic compounds.

When reaction was performed in the presence of the M_1 or M_2 catalyst, upon H_2O_2 addition and UV irradiation, significant degradation of 4-CP during photo-Fenton process was observed.

As shown in Figure 8, Siderite (M_2) exhibited a higher catalytic activity for 4-CP conversion than Hematite (M_1) in the photo-Fenton reaction. Chlorophenol (i.e., 4-CP) removal efficiency of 100% was achieved within 60 min by siderite sample, but longer time of 120 min was required to completely degrade 4-CP with hematite. These results correlated well with the physicochemical properties of those materials due to higher iron content and specific surface area of M_2 sample (Tables 1 and 2). It is well known that complete oxidation (i.e., mineralization) of 4-CP occurred through several intermediate reactions, such as hydroxybenzoquinone (yellow), *o*-benzoquinone (red), and hydroquinone (colorless) and/or maleic and other carboxylic acids, some of them being even more toxic than 4-CP itself [30]. Bel Hadjltaief et al. [10,11] observed yellow color during the degradation of phenol and 2-Chlorophenol using raw and modified clay as catalysts by photo-Fenton process. Brownish color can be assigned to the presence of hydroxybenzoquinone, considered an intermediate in the 4-CP oxidation process.

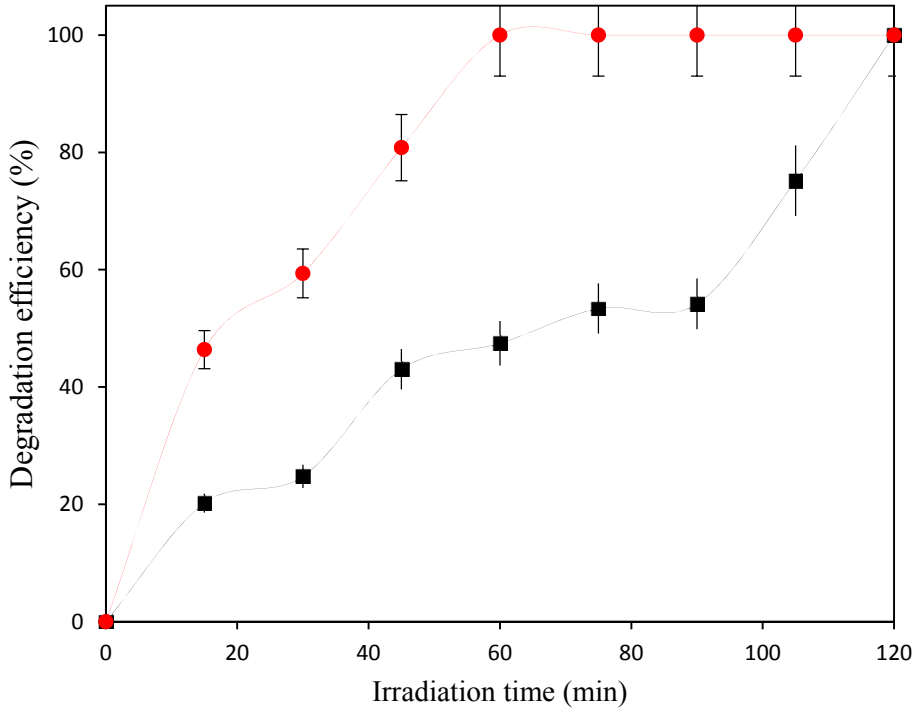

Figure 8. 4-CP degradation efficiency measured using the photo-Fenton experiments at initial 4-CP concentration: 20 mg/L, pH: 3, 0.05 g/L catalyst loading and 2 ml of H_2O_2.

Figure 9 shows the mineralization of 4-CP, measured by TOC analysis under the same experimental conditions as those of Figure 8. TOC reduction rate reached 34.56% for M_1 and 50.05% for M_2 after 120 min of irradiation time. Generally, more than 3 h irradiation time is needed to achieve a complete mineralization of 4-CP. However, shorter time of high efficiencies by M_1 and M_2 samples were recorded, confirming their good catalytic activity in photo-Fenton reaction. On the other hand, after 120 min, iron-leaching was evaluated to 0.081 and 0.079 ppm for M_1 and M_2, respectively (Table 3).

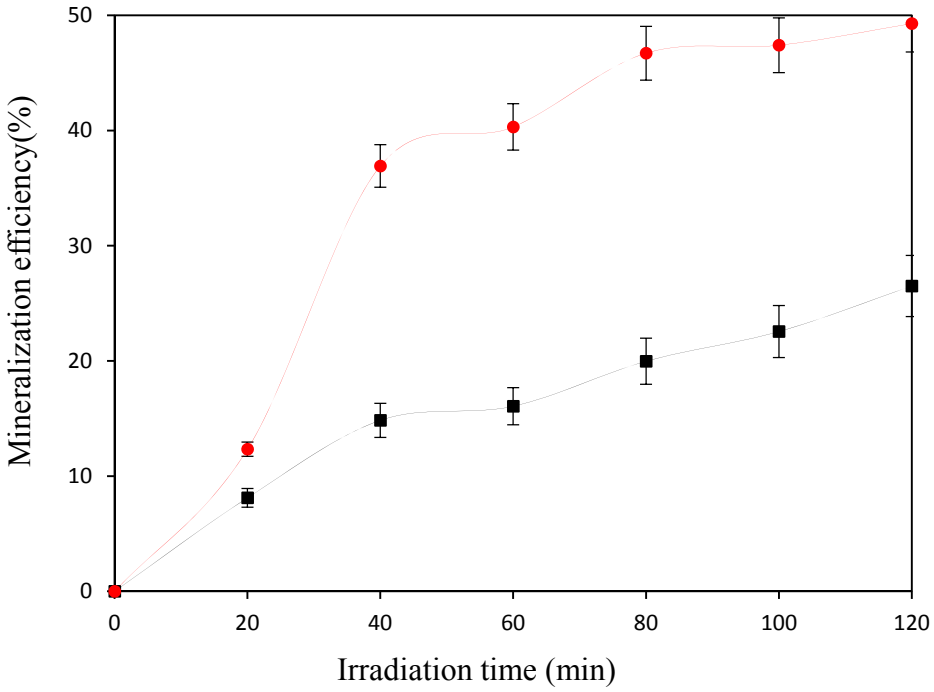

Figure 9. 4-CP mineralization efficiency measured using the photo-Fenton experiments at initial 4-CP concentration: 20 mg/L, pH: 3, 0.05 g/L catalyst loading and 2 mL of H_2O_2.

Table 3. Iron leaching in solution with different reaction time in the both raw materials system.

Iron concentration (ppm)	Samples	Time, min	0	20	40	60	80	100	120
	M_1	0	0.035	0.052	0.060	0.065	0.077	0.080	0.081
	M_2	0	0.028	0.042	0.049	0.056	0.058	0.060	0.079

The effect of temperature on photo-Fenton degradation of 4-CP was also studied in the presence of both catalysts. The kinetic degradation of 4-CP was performed at different temperatures of 20−50 °C. A typical first-order kinetic model was fitted to the experimental results as expressed in Equation (2) [31].

$$\ln\left(\frac{C_0}{C_t}\right) = K_{app} \times t \quad (2)$$

where k_{app} is the apparent rate constant of the first-order reaction (min^{-1}), and C_0 and C_t are the concentrations (mg/L) of the 4-CP at time 0 and t, respectively.

Figure 10a,b shows the plots of 4-CP degradation, corresponding to the fitting of experimental data obtained at different temperatures (20−50 °C) to the apparent-first-order kinetic model. Rate constant, k, can be obtained directly from regression analysis of the linear form of the plot. The coefficient of determination (R^2) for this linear regression ranged 0.9904–0.9958 for M_1 and 0.9953–0.9689 for M_2, indicating a high degree of fitting to the first-order kinetic model.

For both catalysts, the rate constants increased with initial temperature. It was also observed that temperature increase enhanced the hydroxylation rate at the catalyst active sites, resulting in an increased production of •OH radicals. Moreover, a higher reaction temperature can provide more energy for the reactants to go beyond the activation energy barrier [32]. Such an excess energy may lead to higher collision frequency between the •OH radicals and 4-CP molecules (or intermediate), which possibly results in faster degradation process [11].

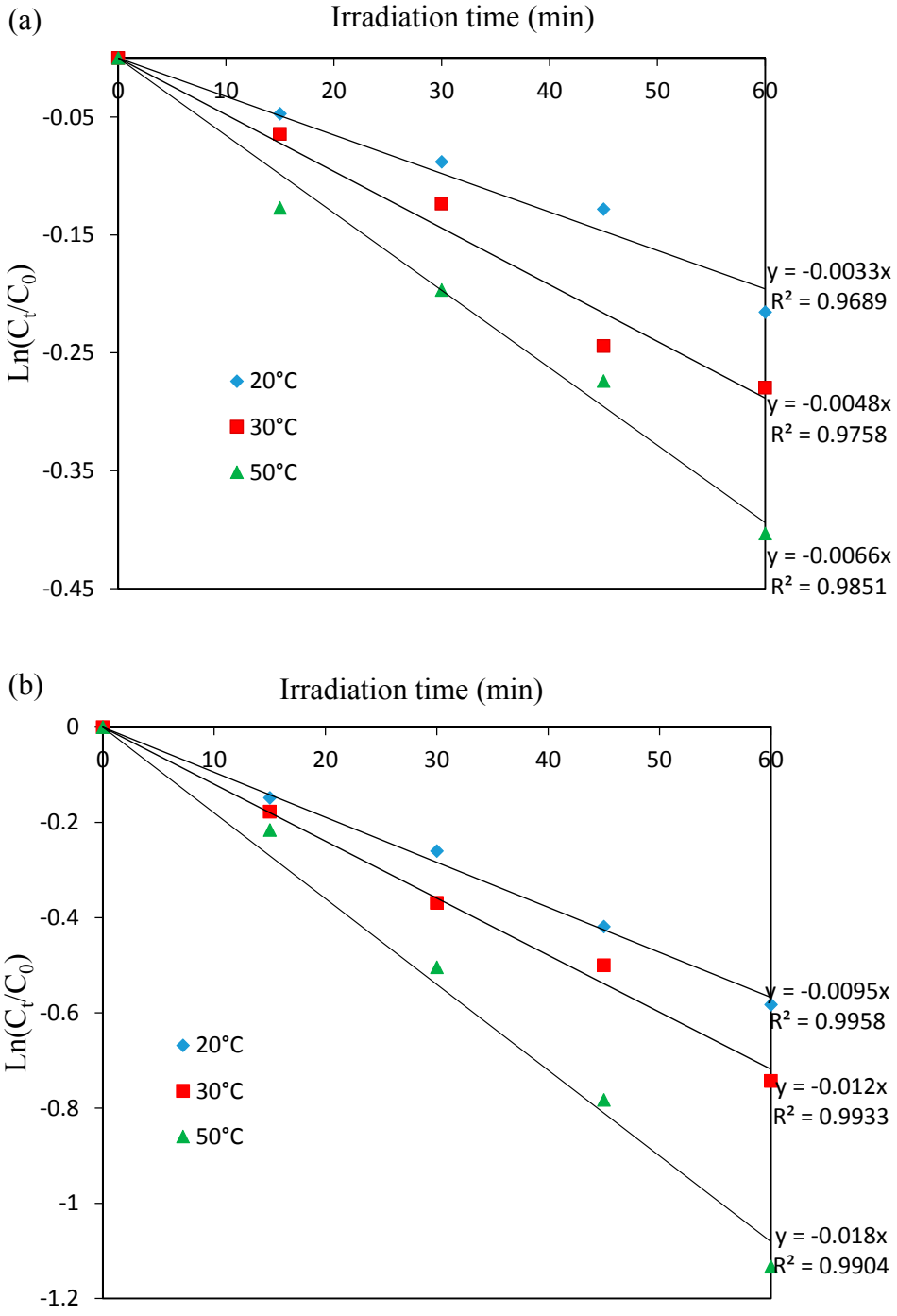

Figure 10. Effect of temperature on the photo-Fenton degradation of 4-CP using: (**a**) M_1; and (**b**) M_2.

The apparent activation energy (E_a) for the degradation of phenol by photo-Fenton oxidation can be calculated from Arrhenius equation as follows:

$$K_{app} = A \cdot \exp(-E_a/RT) \quad (3)$$

The linear form ln (k_{app}) = f($1/T$) gives a straight line, with a slope equal to E_a/R. From the data obtained for all the catalysts, E_a was 32.89 and 36.41 kJ/mol for M_1 and M_2 samples, respectively (Figure 11). This apparent energy represents the total activation energy of photo-Fenton degradation of 4-CP.

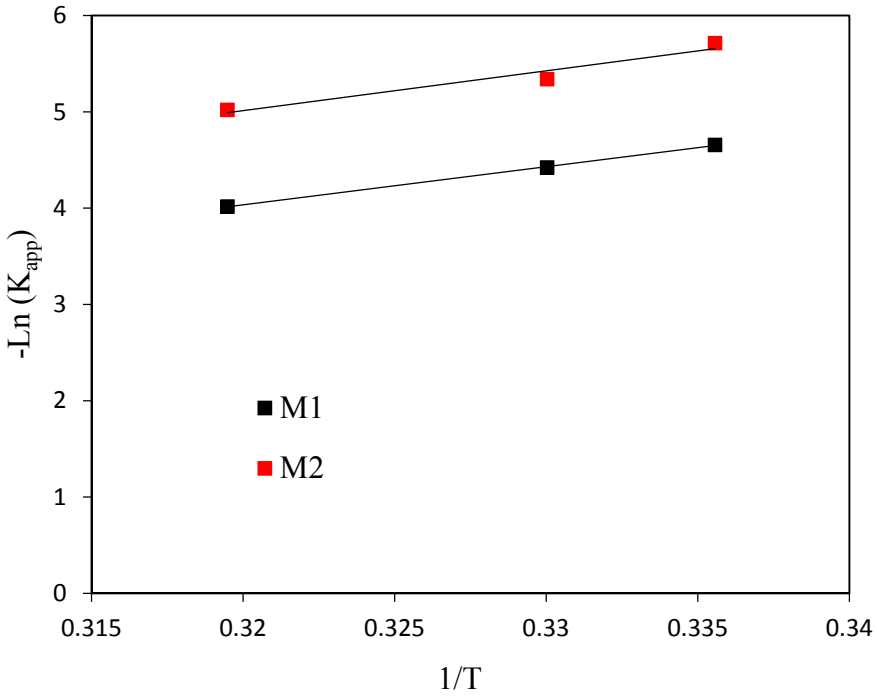

Figure 11. The plots of ln (k_{app}) versus $1/T$, (T is the temperature).

To test the feasibility of cyclic use of the studied raw materials, five photo-Fenton degradation cycles of 4-CP were performed under optimized conditions. At the end of the degradation process, the suspension was centrifuged; the catalyst was washed and dried at 120 °C for subsequent uses. The obtained results are given in Table 4. They showed that 4-CP removal efficiency, during photo-Fenton degradation, decreased with the number of recycling runs. Compared to similar studies, iron leaching was somewhat lower [11,33] confirming the good stability of both supports. The concentration of Fe in the liquid solutions upon the photo-Fenton reaction was found to be at all times lower than 20 ppm.

Table 4. Degradation efficiency through five consecutive catalysts reuse cycles.

Samples	Run Number				
	1	**2**	**3**	**4**	**5**
M_1	100	100	99.87	98.66	98.07
M_2	100	100	100	99.01	98.24

3.3. Comparison of Efficiency of Reaction with Previous Studies

Based on previous relevant studies, a comparative assay was performed to highlight the higher efficiency of the present natural ferruginous materials (i.e., hematite and siderite) in the degradation of 4-CP solute (Table 5). Considering different treatment approaches, such as adsorption, biological treatment, wet oxidation and photodegradation, photo-Fenton process showed more favorable application for the removal of 4-CP than other methods reported in the literature. As can be seen, the obtained maximum 4-CP degradation by raw ferrous samples was higher than those of other catalysts. The high efficiency of our system was related to the high iron on the surface and the nature of catalytic support. For instance, both M_1 and M_2 natural ferrous samples showed full degradation efficiency (100%). This was the highest removal rate when compared to photo-Fenton degradation using iron PILC clay (94%) [8], sunlight-Fenton in ice (80%) [7] and photodegradation [1].

Furthermore, the degradation efficiency of 4-CP by M_1 and M_2 natural samples was much larger than that recorded by Khanikar and Bhattacharyya [4] who found 69% degradation efficiency by Cu-kaolinite and Cu-montmorillonite catalysts via a wet oxidative method. Both hematite and siderite samples have achieved high degradation rate for 4-CP under the experimental conditions of the present study. Therefore, their use as cost-effective catalysts for the removal of 4-chlorophenol in aqueous conditions is a highly recommended option that can be developed into a viable technique.

Table 5. Comparison of degradation efficiency and times for different methods.

Method	Reaction Time (min)	Initial Concentration (mg/L)	Degradation Efficiency (%)	Ref.
Biodegradation	120	10	86	[6]
Adsorption (Activated carbon)	700	100	78.5	[5]
Wet oxidation (Cu-Clays)	480	100	69	[4]
Photodegradation (Cu@AgCl)	40	20	91	[1]
Photo-Fenton	180	100	80	[7]
Photo-Fenton (PILC)	120	100	94	[8]
Photo-Fenton (M_1/M_2)	120	20	100	this work

4. Conclusions

Mined natural Hematite (M_1) and Siderite (M_2) can be effectively used as heterogeneous photo-Fenton catalysts for the degradation of 4-Chlorophenol (4-CP) from aqueous solution. SEM, EDX and XRD analyses confirmed the good structure of these materials as catalysts with high iron content dispersed on the surface. Photo-Fenton degradation process was successfully applied for the removal of 4-Chlorophenol in aqueous conditions. Our results showed that 4-Chlorophenol could be effectively removed from the aqueous media by a heterogeneous photo-Fenton process in the presence of both materials as the catalysts. Moreover, regeneration experiments proved that Siderite had a good stability and reusability, demonstrating the feasibility of using these Tunisian materials for this environmental application. Finally, these pioneering results suggest a further in-depth study for the application of those natural materials as catalysts for the removal of several organic compounds in aqueous conditions. The application of heterogeneous photo-Fenton process and/or Fenton-like process is also appropriate.

Author Contributions: Conceptualization, A.S. and H.B.H.; Methodology, M.E.G. and P.D.C.; Experiments: H.Z.; Formal Analysis, M.E.G., P.D.C. and H.Z.; Interpretation, all authors; Writing—Original Draft Preparation, A.S. and H.B.H.; Writing—Review and Editing, A.S. and H.B.H.; Visualization, X.X.; Supervision, P.D.C. and M.B.Z.; and all authors participated in the discussion of the results and the drafting of the paper.

Funding: This research received no external funding.

Conflicts of Interest: The authors declare no conflict of interest.

References

1. Huang, Z.; Wen, M.; Wu, Q.; Zhang, Y.; Fang, H.; Chen, H. Fabrication of Cu@AgCl nanocables for their enhanced activity toward the catalytic degradation of 4-chlorophenol. *J. Colloid Interface Sci.* **2015**, *460*, 230–236. [CrossRef] [PubMed]
2. Wang, B.; Okoth, O.K.; Yan, K.; Zhang, J. A highly selective electrochemical sensor for 4-chlorophenol determination based on molecularly imprinted polymer and PDDA-functionalized graphene. *Sens. Actuators B Chem.* **2016**, *236*, 294–303. [CrossRef]
3. Chen, X.; Bian, W.; Song, X.; Liu, D.; Zhang, J. Degradation of 4-chlorophenol in a dielectric barrier discharge system. *Sep. Purif. Technol.* **2013**, *120*, 102–109. [CrossRef]

4. Khanikar, N.; Bhattacharyya, K.G. Cu(II)-kaolinite and Cu(II)-montmorillonite as catalysts for wet oxidative degradation of 2-chlorophenol, 4-chlorophenol and 2,4-dichlorophenol. *Chem. Eng. J.* **2013**, *233*, 88–97. [CrossRef]
5. Chen, C.; Geng, X.; Huang, W. Adsorption of 4-chlorophenol and aniline by nanosized activated carbons. *Chem. Eng. J.* **2017**, *327*, 941–952. [CrossRef]
6. Zhang, D.; Deng, M.; Cao, H.; Zhang, S.; Zhao, H. Laccase immobilized on magnetic nanoparticles by dopamine polymerization for 4-chlorophenol removal. *Green Energy Environ.* **2017**, *2*, 393–400. [CrossRef]
7. Liu, J.; Wu, J.Y.; Kang, C.L.; Peng, F.; Liu, H.F.; Yang, T.; Shi, L.; Wang, H.L. Photo-fenton effect of 4-chlorophenol in ice. *J. Hazard. Mater.* **2013**, *261*, 500–511. [CrossRef] [PubMed]
8. Del Campo, E.M.; Romero, R.; Roa, G.; Peralta-Reyes, E.; Espino-Valencia, J.; Natividad, R. Photo-Fenton oxidation of phenolic compounds catalyzed by iron-PILC. *Fuel* **2014**, *138*, 149–155. [CrossRef]
9. Fida, H.; Zhang, G.; Guo, S.; Naeem, A. Heterogeneous Fenton degradation of organic dyes in batch and fixed bed using La-Fe montmorillonite as catalyst. *J. Colloid Interface Sci.* **2017**, *490*, 859–868. [CrossRef] [PubMed]
10. Hadjltaief, H.B.; Sdiri, A.; Ltaief, W.; da Costa, P.; Gálvez, M.E.; Zina, M.B. Efficient removal of cadmium and 2-chlorophenol in aqueous systems by natural clay: Adsorption and photo-Fenton degradation processes. *C. R. Chim.* **2018**, *21*, 253–262. [CrossRef]
11. Hadjltaief, H.B.; da Costa, P.; Beaunier, P.; Gálvez, M.E.; Zina, M.B. Fe-clay-plate as a heterogeneous catalyst in photo-Fenton oxidation of phenol as probe molecule for water treatment. *Appl. Clay Sci.* **2014**, *91–92*, 46–54. [CrossRef]
12. Guo, S.; Zhang, G.; Wang, J. Photo-Fenton degradation of rhodamine B using Fe_2O_3-Kaolin as heterogeneous catalyst: Characterization, process optimization and mechanism. *J. Colloid Interface Sci.* **2014**, *433*, 1–8. [CrossRef] [PubMed]
13. Navalon, S.; Alvaro, M.; Garcia, H. Heterogeneous Fenton catalysts based on clays, silicas and zeolites. *Appl. Catal. B Environ.* **2010**, *99*, 1–26. [CrossRef]
14. Liotta, L.F.; Gruttadauria, M.; di Carlo, G.; Perrini, G.; Librando, V. Heterogeneous catalytic degradation of phenolic substrates: Catalysts activity. *J. Hazard. Mater.* **2009**, *162*, 588–606. [CrossRef] [PubMed]
15. Garrido-Ramírez, E.G.; Theng, B.K.; Mora, M.L. Clays and oxide minerals as catalysts and nanocatalysts in Fenton-like reactions—A review. *Appl. Clay Sci.* **2010**, *47*, 182–192. [CrossRef]
16. Ltaïef, A.H.; Pastrana-Martínez, L.M.; Ammar, S.; Gadri, A.; Faria, J.L.; Silva, A.M.T. Mined pyrite and chalcopyrite as catalysts for spontaneous acidic pH adjustment in Fenton and LED photo-Fenton-like processes. *J. Chem. Technol. Biotechnol.* **2017**, *93*, 1137–1146. [CrossRef]
17. Changotra, R.; Rajput, H.; Dhir, A. Natural soil mediated photo Fenton-like processes in treatment of pharmaceuticals: Batch and continuous approach. *Chemosphere* **2017**, *188*, 345–353. [CrossRef] [PubMed]
18. Minella, M.; Marchetti, G.; de Laurentiis, E.; Malandrino, M.; Maurino, V.; Minero, C.; Vione, D.; Hanna, K. Photo-Fenton oxidation of phenol with magnetite as iron source. *Appl. Catal. B Environ.* **2014**, *154–155*, 102–109. [CrossRef]
19. El Mehdi Benacherine, M.; Debbache, N.; Ghoul, I.; Mameri, Y. Heterogeneous photoinduced degradation of amoxicillin by Goethite under artificial and natural irradiation. *J. Photochem. Photobiol. A Chem.* **2017**, *335*, 70–77. [CrossRef]
20. Djeffal, L.; Abderrahmane, S.; Benzina, M.; Fourmentin, M.; Siffert, S.; Fourmentin, S. Efficient degradation of phenol using natural clay as heterogeneous Fenton-like catalyst. *Environ. Sci. Pollut. Res. Int.* **2013**, *21*, 3331–3338. [CrossRef] [PubMed]
21. Bel Hadjltaief, H.; Zina, M.B.; Galvez, M.E.; da Costa, P. Photo-Fenton oxidation of phenol over a Cu-doped Fe-pillared clay. *C. R. Chim.* **2015**, *18*, 1161–1169. [CrossRef]
22. Bel Hadjltaief, H.; da Costa, P.; Galvez, M.E.; Zina, M.B. Influence of operational parameters in the heterogeneous photo-fenton discoloration of wastewaters in the presence of an iron-pillared clay. *Ind. Eng. Chem. Res.* **2013**, *52*, 16656–16665. [CrossRef]
23. Zou, X.; Chen, T.; Liu, H.; Zhang, P.; Chen, D.; Zhu, C. Catalytic cracking of toluene over hematite derived from thermally treated natural limonite. *Fuel* **2016**, *177*, 180–189. [CrossRef]
24. Acisli, O.; Khataee, A.; Soltani, R.D.C.; Karaca, S. Ultrasound-assisted Fenton process using siderite nanoparticles prepared via planetary ball milling for removal of reactive yellow 81 in aqueous phase. *Ultrason. Sonochem.* **2017**, *35*, 210–218. [CrossRef] [PubMed]

25. Zhao, K.; Guo, H.; Zhou, X. Adsorption and heterogeneous oxidation of arsenite on modified granular natural siderite: Characterization and behaviors. *Appl. Geochem.* **2014**, *48*, 184–192. [CrossRef]
26. Selmani, S.; Essaidi, N.; Gouny, F.; Bouaziz, S.; Joussein, E.; Driss, A.; Sdiri, A.; Rossignol, S. Physical-chemical characterization of Tunisian clays for the synthesis of geopolymers materials. *J. Afr. Earth Sci.* **2015**, *103*, 113–120. [CrossRef]
27. Eloussaief, M.; Benzina, M. Efficiency of natural and acid-activated clays in the removal of Pb(II) from aqueous solutions. *J. Hazard. Mater.* **2010**, *178*, 753–757. [CrossRef] [PubMed]
28. Sdiri, A.; Higashi, T.; Hatta, T.; Jamoussi, F.; Tase, N. Mineralogical and spectroscopic characterization, and potential environmental use of limestone from the Abiod formation, Tunisia. *Environ. Earth Sci.* **2010**, *61*, 1275–1287. [CrossRef]
29. Sdiri, A.; Higashi, T.; Jamoussi, F.; Bouaziz, S.; Hatta, T.; Jamoussi, F.; Tase, N.; Bouaziz, S. Effects of impurities on the removal of heavy metals by natural limestones in aqueous systems. *J. Environ. Manag.* **2012**, *93*, 171–179. [CrossRef] [PubMed]
30. Mijangos, F.; Varona, F.; Villota, N. Changes in solution color during phenol oxidation by fenton reagent. *Environ. Sci. Technol.* **2006**, *40*, 5538–5543. [CrossRef] [PubMed]
31. Niu, P.; Hao, J. Efficient degradation of organic dyes by titanium dioxide–silicotungstic acid nanocomposite films: Influence of inorganic salts and surfactants. *Colloids Surf. A Physicochem. Eng. Asp.* **2014**, *443*, 501–507. [CrossRef]
32. Xu, H.Y.; Prasad, M.; Liu, Y. Schorl: A novel catalyst in mineral-catalyzed Fenton-like system for dyeing wastewater discoloration. *J. Hazard. Mater.* **2009**, *165*, 86–92.
33. Bel Hadjltaief, H.; Zina, M.B.; da Costa, P.; Gálvez, M.E. Heterogeneous TiO_2–Fe-plate catalyst for the discoloration and mineralization of aqueous solutions of cationic and anionic dyes. *Desalination Water Treat.* **2015**, *57*, 13505–13517. [CrossRef]